



Linearized Mathematical Model for PWR Dynamics Simulation

Nehad A. Demerdash¹, Mohamed A. El-Hameed², Mahdy M. El-Arini², Ezzat A. Eisawy¹

(¹) Egyptian Nuclear & Radiological Regulatory Authority, Nasr City P.O. Box7551, Cairo, Egypt.

(²) Electrical Power and Machines Department, Zagazig University, Zagazig 44519, Egypt

Received 28th Oct. 2019
Accepted 17th Nov. 2019

A linearized mathematical model for the pressurized water reactor (PWR) nuclear power plant dynamics simulation is presented based on conservation of energy and mass balance. The core and coolant system are treated as a lumped parameter. The delayed neutrons effect is considered. The model state variables are linearized in first order differential equations with steady state initial values. The reactor core dynamic response is investigated through transients represented in external reactivity insertion e.g.(0.001 $\Delta k/k$), 10% step decrease in core flow rate and 10 °F step decrease in core inlet coolant temperature. The simulation results demonstrated the role of feedback reactivity form coolant temperature and Doppler Effect in stabilizing the core power and affecting the steady state values of core variables.

Keywords: Nuclear power plant / Pressurized water reactor / Reactor simulation / Feedback, reactor dynamics

Introduction

Nuclear energy is considered as one of the most important sources of a clean and cheap energy. Therefore, there is a need to investigate the safety and stability of nuclear power plants. Safety issues have two main aspects, stability of plant under physical and thermal transients and stability of plant following the power grid disturbances. This paper focuses on the reactor core stability subjected to input transients. As it is difficult to perform this study practically, the need arises to model the reactor core and simulate it to monitor the reactor reaction under the different transients. Reactor simulation modeling is handled previously in published papers. In [1] a pressurized water reactor model was

proposed and implemented through a user-defined program in PSASP where, the dynamics of the reactor due to common step disturbances in reactivity and coolant temperature were simulated. The model simulation clarified the importance of feedbacks to reactor stability. The same reactor model for dynamic analysis [2] was implemented by Scilab where, the response of core variables to perturbations in reactivity, inlet coolant temperature and primary coolant flow rate were presented. The author assessed the results by PWR model developed in [3] depending on the positive reactivity perturbation and the differences were attributed to different design values and thermal hydraulic

Corresponding author: nehadali_2004@yahoo.com

DOI: [10.21608/ajnsa.2019.18780.1290](https://doi.org/10.21608/ajnsa.2019.18780.1290)

© Scientific Information, Documentation and Publishing Office (SIDPO)-EAEA

conditions. Also, the same reactor model was introduced in many published papers as a part of the whole PWR nuclear power plant for the purpose of studying dynamic characteristics of PWR [4] or power system analysis as in [5-6]. In a recent work [7] the dynamics simulation approach by adopting reactor model to investigate the thermal dynamic processes is presented. This model was validated using results from published work in

[8]. In the present work, a reactor model suitable for the dynamic analysis is proposed, in which the feedback from coolant temperature and fuel temperature effects are considered to model the true characteristics of the reactor. The model is implemented and the reactor dynamics can be easily investigated through perturbations applied to control input parameter.

Nomenclature

A_{fC}	Effective heat transfer surface area between the reactor fuel and primary coolant, (ft ²).	PSAP	Power System Analysis Software Package
C_i	Precursor concentration for the i th precursor group, $i=1, \dots, 6$	Scilab	A numerical computational high level software
C_{PC}	Reactor coolant specific heat, (Btu/lb.°F).	T_{LP}	Primary coolant temperature in reactor lower plenum, (°F)
C_{Pf}	Reactor fuel specific heat, (Btu/lb.°F)	T_{UP}	Primary coolant temperature in reactor upper plenum, (°F)
F_r	Fraction of total power generated in fuel.	U_{fC}	Heat transfer coefficient from fuel to coolant
M_f	Mass of reactor fuel, (lb).	W_{PRIM}	Primary coolant mass flow rate inside the core.
M_C	Mass of reactor coolant, (lb)	β_t	Total delayed neutron fraction, $\beta_t = \sum_1^6 \beta_i$
M_{LP}	Mass of coolant in lower plenum, (lb).	β_i	Delayed neutron fraction for the six delayed-neutron groups, $i=1, \dots, 6$
M_{HL}	Mass of coolant in hot leg, (lb)	Λ	Neutron generation time, (s).
P_r	Normalized core thermal power	α_f	Fuel temperature coefficient of reactivity, (1/oF)
P	Reactor thermal power, (MWth).	α_c	Coolant temperature coefficient of reactivity, (1/°F)
P_0	Initial reactor thermal power, (MWth).	λ_i	Delayed neutron group decay constant, 1/s
T_f	Average fuel temperature, (°F)	ρ_{ext}	External reactivity due to control rod movement
T_{f0}	Average initial fuel temperature, (°F)	ρ_0	Initial value of core reactivity
T_{C1}	Primary coolant temperature at lump1, (°F)		
T_{C2}	Primary coolant temperature at lump2, (°F)		
T_{C0}	Primary coolant average temperature, (°F)		
T_{CL}	Primary coolant temperature in cold-leg, (°F)		
T_{PSGO}	Temperature of primary coolant out from steam generator, (°F).		
T_{HL}	Primary coolant temperature in hot-leg, (°F)		

Plant Dynamic Model

The plant dynamic model is structured in a way to include reactor neutron dynamic, reactor thermodynamic, plant components such as reactor plenums and piping. Plant state variables are represented by first order differential equations based on the conservation of mass and energy laws. Reactor neutron dynamic is modeled by using the

point kinetic equation with six groups of delayed neutrons and the reactivity feedback from fuel and coolant temperatures are considered in total reactivity. It is assumed that the spatial distribution shape of the neutron flux density do not change during the transients [9-11].

Reactor Kinetics Model

$$\frac{dP_r(t)}{dt} = \left(\frac{\rho(t) - \beta_t}{\Lambda} \right) * P_r(t) + \sum_{i=1}^6 \lambda_i * \text{Crit}, P_r = PPO \quad (1)$$

$$\frac{dC_{ri}(t)}{dt} = \frac{\beta_i}{\Lambda} P_r(t) - \lambda_i C_{ri}(t), \quad i = 1:6 \quad (2)$$

B. Reactor Core thermal dynamic model

The core heat transfer model utilizes mann's [10] approximation for fuel and coolant temperatures as shown in Figure (1). Two well stirred coolant nodes are used for each fuel node to obtain a good approximation to the heat transfer driving force between fuel and coolant.

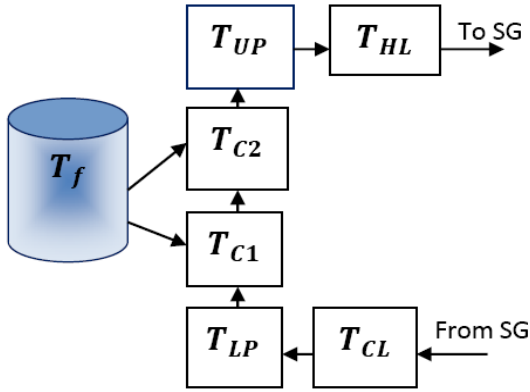


Figure (1): Schematic diagram of reactor thermal model lumps

$$\frac{dT_f}{dt} = \frac{F_r P_0}{M_f C_{Pf}} P_r - \frac{U_{fC} A_{fC}}{M_f C_{Pf}} T_f + \frac{U_{fC} A_{fC}}{2M_f C_{Pf}} T_{C1} + \frac{U_{fC} A_{fC}}{2M_f C_{Pf}} T_{C2} \quad (3)$$

$$\frac{dT_{C1}}{dt} = \frac{(1 - F_r) P_0}{M_C C_{PC}} P_r + \frac{U_{fC} A_{fC}}{M_C C_{PC}} (T_f - T_{C1}) + \left(\frac{W_{PRIM}}{M_C} \right) (T_{LP} - T_{C1}) \quad (4)$$

$$\frac{dT_{C2}}{dt} = \frac{(1 - F_r) P_0}{M_C C_{PC}} P_r + \frac{U_{fC} A_{fC}}{M_C C_{PC}} (T_f - T_{C1}) + \left(\frac{W_{PRIM}}{M_C} \right) (T_{C1} - T_{C2}) \quad (5)$$

C. Core reactivity

The total reactivity in the core is represented by the initial value of reactivity in core and external reactivity caused by a change in rod movement and reactivity feedback induced by change in fuel temperature (Doppler Effect), and by change in coolant temperature.

$$\rho(t) = \rho_0 + \rho_{ext} + \alpha_f * (T_f - T_{f0}) + \alpha_c * (T_C - T_{C0}) \quad (6)$$

D. Reactor Piping and Plenums

In reactor plenums, Figure (1), complete mixing is assumed during normal transients. The energy conservation equation are applied on both plenums, this will result in two first order lag equations for the upper and lower plenum temperatures.

$$\frac{dT_{LP}}{dt} = \frac{W_{PRIM}}{M_{LP}} (T_{CL} - T_{LP}) \quad (7)$$

$$\frac{dT_{UP}}{dt} = \frac{W_{PRIM}}{M_{UP}} (T_{C2} - T_{UP}) \quad (8)$$

$$\frac{dT_{CL}}{dt} = \frac{W_{PRIM}}{M_{CL}} (T_{PSGO} - T_{CL}) \quad (9)$$

$$\frac{dT_{HL}}{dt} = \frac{W_{PRIM}}{M_{HL}} (T_{UP} - T_{HL}) \quad (10)$$

The above-mentioned equations are linearized with reference to the steady state initial values and presented in state space form as shown in equations (11)

$$\dot{X}_R = A_R * X_R + B_R * U_R \quad (11)$$

Where, \dot{X}_R : Reactor state variables vector, A_R : Reactor coefficient matrix, B_R : Coefficient of reactor input matrix, U_R : Reactor input variables

vector. Equation (11) can be detailed to represent PWR reactor state space model as follows:

$$\begin{bmatrix} \frac{d\Delta P_r}{dt} \\ \frac{d\Delta C_{r1}}{dt} \\ \frac{d\Delta C_{r2}}{dt} \\ \frac{d\Delta C_{r3}}{dt} \\ \frac{d\Delta C_{r4}}{dt} \\ \frac{d\Delta C_{r5}}{dt} \\ \frac{dT_{f1}}{dt} \\ \frac{dT_{f2}}{dt} \\ \frac{dT_{f3}}{dt} \\ \frac{dT_{f4}}{dt} \\ \frac{dT_{f5}}{dt} \\ \frac{dT_{f6}}{dt} \\ \frac{dT_{f7}}{dt} \\ \frac{dT_{f8}}{dt} \end{bmatrix} = \begin{bmatrix} A_{11} & A_{12} & A_{13} & A_{14} & A_{15} & A_{16} & A_{17} & A_{18} & A_{19} & A_{20} & 0 & 0 & 0 & 0 \\ A_{21} & A_{22} & 0 & 0 & 0 & 0 & 0 & 0 & 0 & 0 & 0 & 0 & 0 & 0 \\ A_{31} & 0 & A_{32} & 0 & 0 & 0 & 0 & 0 & 0 & 0 & 0 & 0 & 0 & 0 \\ A_{41} & 0 & 0 & A_{44} & 0 & 0 & 0 & 0 & 0 & 0 & 0 & 0 & 0 & 0 \\ A_{51} & 0 & 0 & 0 & A_{55} & 0 & 0 & 0 & 0 & 0 & 0 & 0 & 0 & 0 \\ A_{61} & 0 & 0 & 0 & 0 & A_{66} & 0 & 0 & 0 & 0 & 0 & 0 & 0 & 0 \\ A_{71} & 0 & 0 & 0 & 0 & 0 & A_{77} & 0 & 0 & 0 & 0 & 0 & 0 & 0 \\ A_{81} & 0 & 0 & 0 & 0 & 0 & A_{88} & A_{89} & A_{90} & 0 & 0 & 0 & 0 & 0 \\ A_{91} & 0 & 0 & 0 & 0 & 0 & A_{99} & A_{99} & 0 & 0 & 0 & 0 & A_{913} & 0 \\ A_{101} & 0 & 0 & 0 & 0 & 0 & 0 & A_{1010} & A_{1011} & 0 & 0 & 0 & 0 & 0 \\ 0 & 0 & 0 & 0 & 0 & 0 & 0 & 0 & 0 & A_{1111} & A_{1111} & 0 & 0 & 0 \\ 0 & 0 & 0 & 0 & 0 & 0 & 0 & 0 & 0 & 0 & A_{1211} & A_{1211} & 0 & 0 \\ 0 & 0 & 0 & 0 & 0 & 0 & 0 & 0 & 0 & 0 & 0 & A_{1311} & A_{1311} & 0 \\ 0 & 0 & 0 & 0 & 0 & 0 & 0 & 0 & 0 & 0 & 0 & 0 & 0 & A_{1411} \end{bmatrix} \times \begin{bmatrix} \Delta P_r \\ \Delta C_{r1} \\ \Delta C_{r2} \\ \Delta C_{r3} \\ \Delta C_{r4} \\ \Delta C_{r5} \\ \Delta T_{f1} \\ \Delta T_{f2} \\ \Delta T_{f3} \\ \Delta T_{f4} \\ \Delta T_{f5} \\ \Delta T_{f6} \\ \Delta T_{f7} \\ \Delta T_{f8} \end{bmatrix} + \begin{bmatrix} B_{11} & 0 & 0 \\ 0 & 0 & 0 \\ 0 & 0 & 0 \\ 0 & 0 & 0 \\ 0 & 0 & 0 \\ 0 & 0 & 0 \\ 0 & 0 & R_{14} \\ 0 & 0 & R_{13} \end{bmatrix} \times \begin{bmatrix} \Delta \rho_{ext} \\ \Delta T_{P5500} \\ \Delta W_{PRIM} \end{bmatrix}$$

Elements of matrix A and matrix B are listed in details in appendix A. The block diagram for the reactor state space model is shown in (Figure 2).

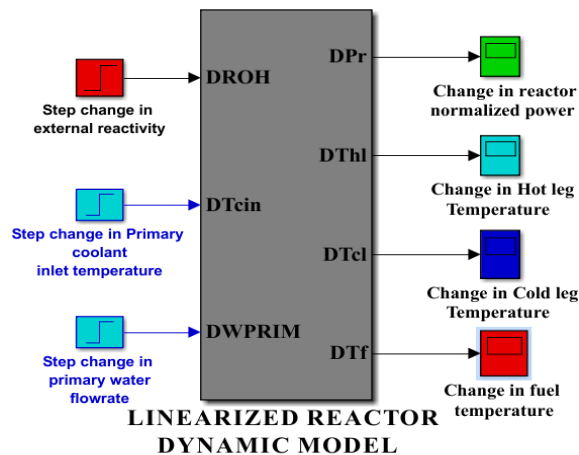


Figure (2): Block diagram of reactor state space model

Simulation of reactor dynamics

The reference plant for developed reactor model is a typical Westinghouse PWR system with thermal energy power 3436 MWth. The technical parameters required for construction of the reactor model are listed in table (1) and delayed neutron data are listed in table (2), [12-13].

Table (1): Reference PWR technical parameter.

Parameter	Value
Nominal Power Output (MWth) thermal power	3436
Fraction of Total Power Generated in Fuel.	0.974
Mass of Fuel (Ibm).	222739
Total Coolant Mass Flow Rate (Ibm/hr)	1.5x10 ⁸
Effective Heat Transfer Area (ft ²).	59900
Specific Heat Capacity of Fuel (btu/Ibm-°F).	0.059
Specific Heat Capacity of Moderator (btu/Ibm -°F).	1.39
Average Overall Heat Transfer Coefficient (btu/Ibm-ft ²).	200

Table (2): Six group delayed neutron data.

Group	Delay Neutron Fraction	Decay Constant
First	β ₁ =0.000209	λ ₁ = 0.012500s ⁻¹
Second	β ₂ =0.001414	λ ₂ =0.030800 s ⁻¹
Third	β ₃ =0.001309	λ ₃ =0.114000 s ⁻¹
Fourth	β ₄ =0.002727	λ ₄ =0.307000 s ⁻¹
Fifth	β ₅ =0.000925	λ ₅ =1.190000s ⁻¹
Sixth	β ₆ =0.006898	λ ₆ =3.190000s ⁻¹

Three different cases of transient are simulated in this study to examine reactor dynamics:-

- Step reactivity increase
- Decrease in inlet core coolant Temperature
- Decrease in primary coolant flow rate

RESULTS

In the following a summary of the reactor core dynamic response results for the simulated transient cases are presented:-

A. Reactor Response for Step Reactivity Increase

A sudden reactivity increase can be due to a control rod withdrawal or a boron dilution or a sudden pump start up. Such event had been simulated by adding a (0.001 Δk/k (i.e., 0.15\$) as a step increase in the core reactivity, (Figure 3(d)). Accordingly, fission rate increases resulting in neutron flux increase, and correspondingly, reactor thermal power rises sharply

to a value of about 15% from rated power. As the reactor power generation increases, the fuel temperature will increase to a value of 50 °F in 5 seconds, from the simulation time, this means that there is a delay between fuel temperature and power increase (Figure 3(b)). The increase in fuel temperature, leads to more heat generated in core which is transferred to the coolant, rising its temperature as shown in (Figure 3(b)). The temperatures of the two coolant modeled lumps, e.g. ΔT_{c1} & ΔT_{c2} , rises to a value of 1.44°F, and 2.76°F,

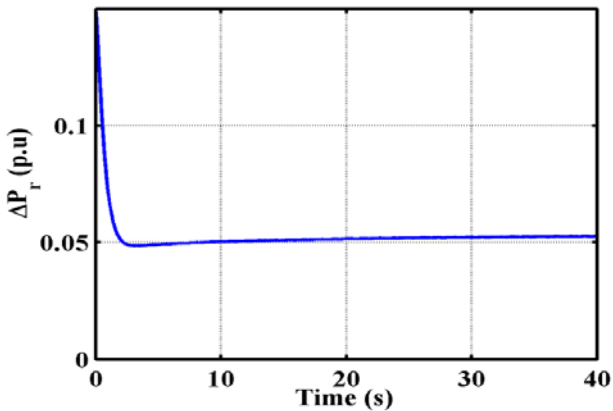


Figure 3(a) Change in reactor normalized thermal power.

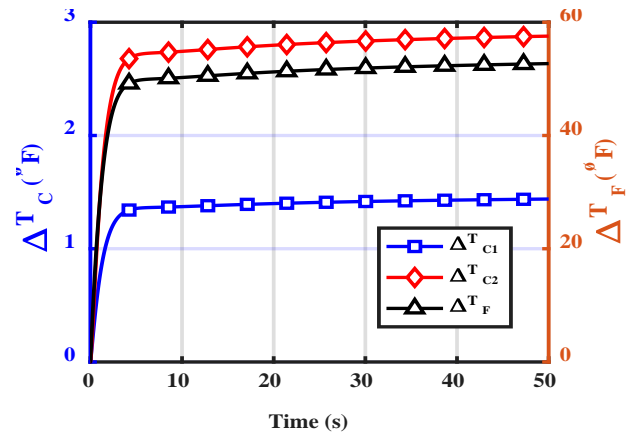


Figure 3(b) Change in fuel and coolant temperature.

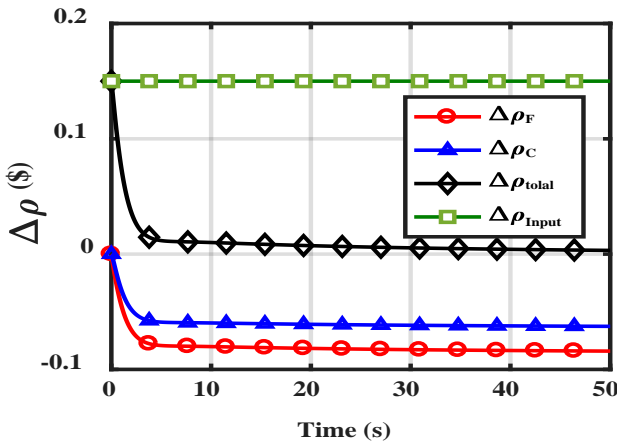


Figure 3(c) Change in core reactivity components.

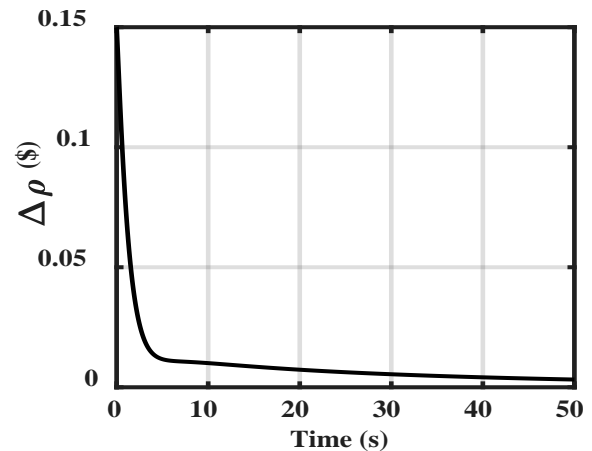


Figure 3(d) Total change in core reactivity.

Figure (3): Reactor variable dynamic response for a step increase in reactivity

B. Dynamics for a Decrease in Inlet Coolant Temperature

The sudden decrease in coolant inlet temperature case is simulated by assuming sudden 10°F step decrease in the core inlet coolant

temperature. The rise in fuel temperature produce negative reactivity (Doppler Effect) of (- 0.08405\$) as shown in (Figure 3(c)). Also, the increase in coolant temperature produces negative reactivity feedback of (- 0.06259\$) as shown in (Figure 3(c)) then the total change in core reactivity decreases as shown in (Figure 3(d)). The reactor reaches a new stable operating condition with an increase in power level relative to steady state value of 0.0534 from the normalized reactor power (Figure 3(a)).

temperature. This is performed to simulate the reactor behavior when the load demand increases and the steam drawn from steam generator increase. Hence, the temperature of primary coolant out from steam generator and inlet to the reactor core decreases. To perform this transient a 10°F step

decrease is applied to the core inlet coolant temperature. This perturbation leads to a decrease in the temperature of the two coolant lumps, e.g. ΔT_{c1} & ΔT_{c2} , to a value of -7.15 °F and -4 °F (Figure 4(b)) respectively. As the coolant temperature decrease it results in positive reactivity in the core (Figure 4(c)). The positive reactivity increases the neutron flux, hence, the reactor power increases rapidly in 6.56 sec by a value of about 11.15% (i.e. 382.5 MW) (Figure 4(a)). Correspondingly, as power increases the fuel temperature increases gradually

until reaching steady state increase of 100 °F (Figure 4(b)). Also, the increase in fuel temperature produces negative reactivity in the core which results in a delay time to the coolant positive reactivity at time of 10 sec as in (Figure 4(c)). The positive feedback reactivity from coolant temperature is 0.1663 (\$) and negative reactivity from Doppler Effect is $[-0.1357$ (\$)]. The resultant change in core reactivity is shown in (Figure 4(d)). As the change in core reactivity goes to zero the reactor stabilizes at new operating conditions.

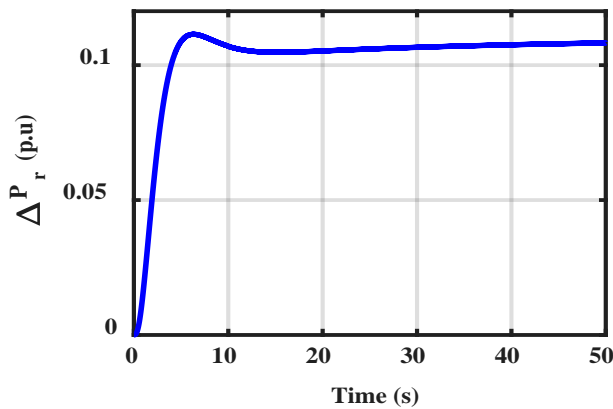


Figure 4(a) Change in reactor normalized thermal power.

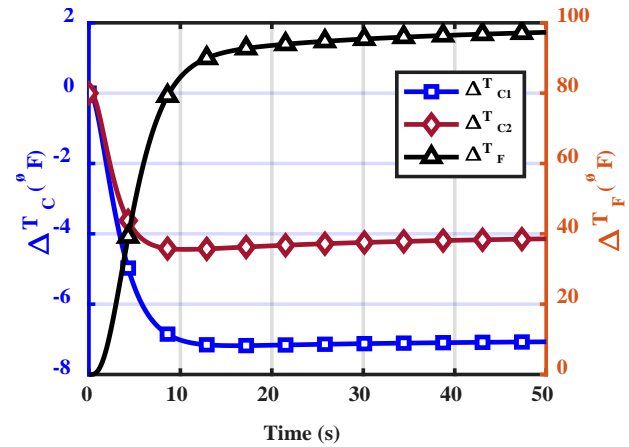


Figure 4(b) Change in fuel and coolant temperature.

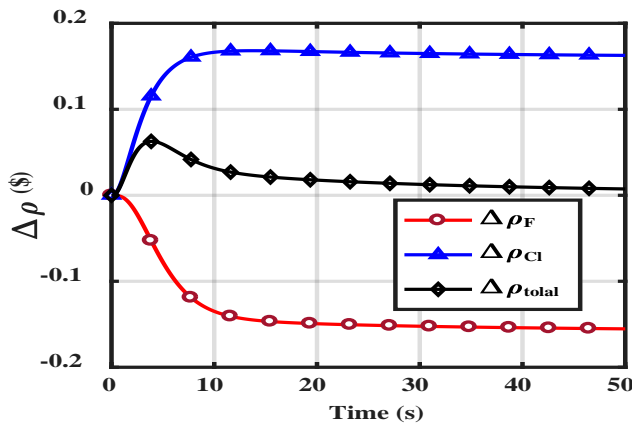


Figure 4(c) Change in core reactivity components.

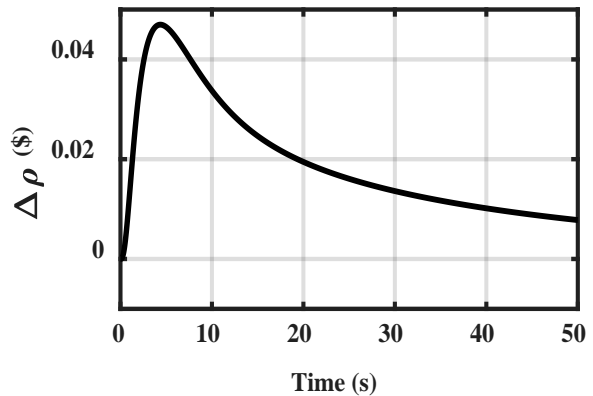


Figure 4(d) Change in core total reactivity.

Figure (4): The dynamic response of reactor parameters for a step decrease to coolant inlet temperature.

C. Dynamics with decrease in primary coolant flow rate due to grid frequency change.

A reactor model is developed to simulate the reactor response due to change in grid frequency

which results in a change in mechanical rotational speed of reactor coolant pumps and accordingly a reduction in the primary coolant flow rate. In this model, 10% decrease in the primary cooling reactor cooling water is considered to occur as a result of change in frequency. This decrease results in a sharp

increase in the temperature of two coolant lumps, e.g. ΔT_{c1} & ΔT_{c2} , in the first two seconds as shown in (Figure 5(b)). This sharp increase produces negative reactivity component in core as shown in (Figure 5(c)) and causes a sharp decrease in reactor power (Figure 5(a)) at a 0.69 sec. The reactor power decreases by -0.0755 of rated power and stabilize at -

0.034 of rated power after about 30 sec. The fuel temperature follows the power reduction and decreases by about 30.52 °F as shown in (Figure 5(b)) and correspondingly, a positive feedback reactivity component is produced in core (Figure 5(c)). The resultant change in core reactivity reaches stable state at -0.005 \$ in 50 sec, (Figure 5(d)).

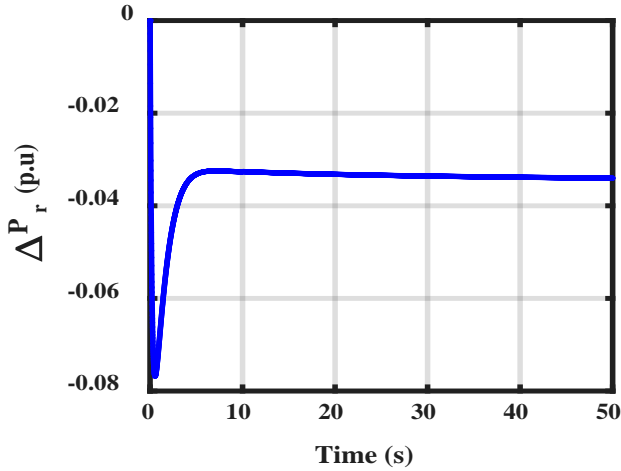


Figure 5(a) Change in reactor normalized thermal power.

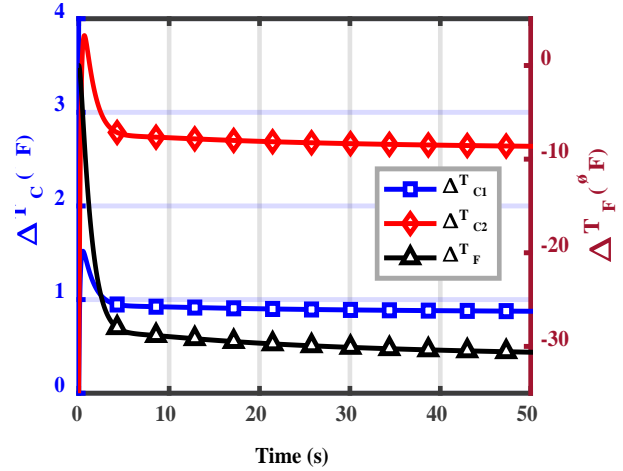


Figure 5(b) Change in fuel and coolant temperature.

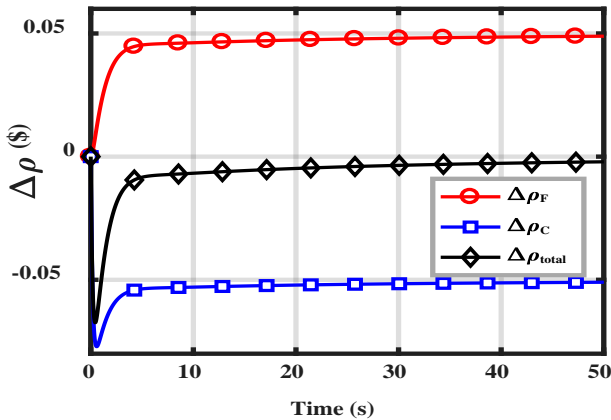


Figure 5(c) Change in core reactivity components.

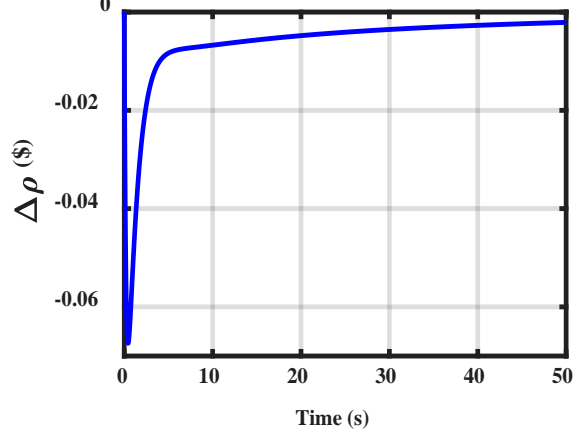


Figure 5(d) Change in core total reactivity.

Figure (5): The dynamic response of reactor parameters for a step decrease in primary coolant flow rate.

Model Validation

A comparison of reactor core dynamic simulations between the developed model results and previously published results in reference [2] are considered. A case of comparison will be made with reference [2]. Considering the case of positive reactivity insertion, the comparison between

normalized power in reference [2] and the presented model is shown in (Figure 6(a)). In both models the transient change in power is the same but for the steady state the value of reference [2] power is higher by about 1.5% of rated power. This may be attributed to difference in values of feedback reactivity from fuel and coolant temperatures which minimize the power increase. Also a fuel

temperature comparison is presented in (Figure 6(b)) where, the fuel temperature increases in the first 5sec to about 50°F in both models. While, in the present model the fuel temperature remained in the same range since the change in core power stabilizes

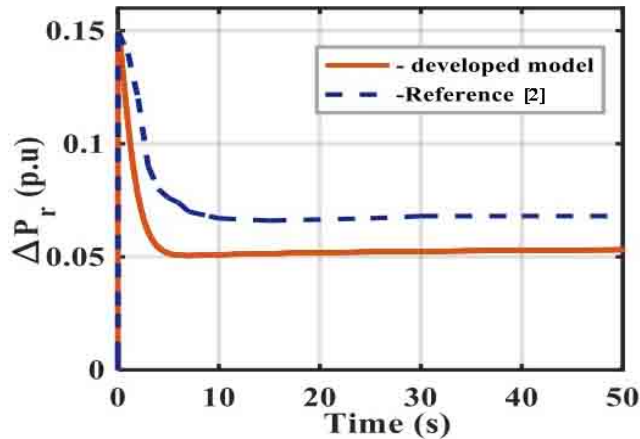


Figure 6(a) Change in normalized reactor thermal power.

after 5 sec, (Figure 6(a)). But for reference [2] the fuel temperature decreases about 5°F after 5 sec. It should be noted that the differences can be attributed to some differences in design parameter values.

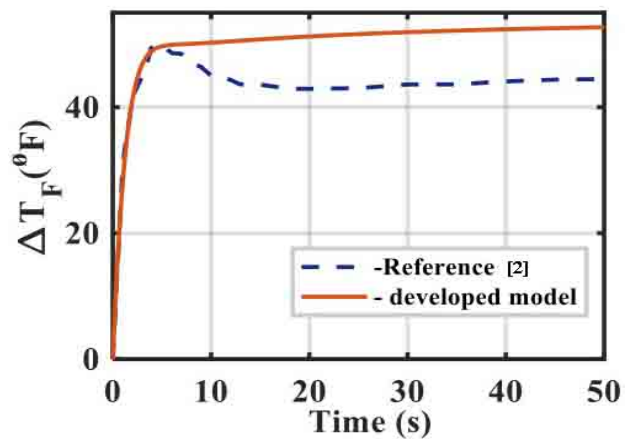


Figure 6(b) Change in fuel temperature.

Figure (6): Comparison between reference simulation and developed model for a change in reactor normalized power and fuel temperature.

Conclusion

In this work a linearized dynamic model for a PWR nuclear power plant core is developed. The dynamic response of reactor core is studied through transient perturbations introduced to the core input parameters. The main points in conclusion are:

- The main role of feedback reactivity from coolant temperature and Doppler Effect is demonstrated as it stabilizes the core power and affects the steady state values.
- The PWR core dynamics is investigated through three different simulated cases of perturbations to reactor model input variables, such as insertion of external reactivity, decrease in primary coolant flow rate and primary coolant inlet temperature.
- The results of the simulated cases are verified by comparison with previously published results which confirm the adequacy of the developed model.

References

1. Shi, X., Wu, P., Liu, D., Li, X., Zhao, J., Zhang, Y., & Zhao, Z., (2009) "Modeling and Dynamic Analysis of Nuclear Power Plant Reactor Based on PSASP", Asia-Pacific Power and Energy Engineering Conference, Proceedings: March 28-31, 2009. IEEE Power & Energy Society.
2. Tsai CW, Shih C, Wang JR., (2013) "Construction of an elementary model for the dynamic analysis of a pressurized water reactor", Transactions of the Canadian Society for Mechanical Engineering 37(3): 603–610. doi:10.4028/www.scientific.net/AMM.284-287.652.
3. Marseguerra, Marzio, Enrico Zio, and Raffaele Canetta. (2004) "Using Genetic Algorithms for Calibrating Simplified Models of Nuclear Reactor Dynamics." Annals of Nuclear Energy 31(11): 1219–50.
4. Xiong L, Liu D, Wang B, Wu P, Zhao J, Shi X., (2009) "Dynamic Characteristics Analyse of Pressurized Water Reactor Nuclear Power Plant Based on PSASP." In 4th IEEE Conference on Industrial Electronics and Applications, ICIEA 2009, 3629–34.
5. Zhao, Jie, Ping Wu, and Dichen Liu. (2009) "User-Defined Modeling of Pressurized Water Reactor Nuclear Power Plant Based on PSASP

- and Analysis of Its Characteristics.” In 2009 Asia-Pacific Power and Energy Engineering Conference, IEEE, 1–6. <http://ieeexplore.ieee.org/document/4918953/>.
6. Gao H, Wang C, Pan W., (2006) “A detailed nuclear power plant model for power system analysis based on PSS/E”, In 2006 IEEE PES Power Systems Conference and Exposition, PSCE 2006 - Proceedings, , 1582–86. doi:10.1109/PSCE.2006.296149.
 7. El-Sefy M., Ezzeldin M., El-Dakhakhni M., Wiebe W., Nagasaki, L. and Mohamed S. (2019) “System Dynamics Simulation of the Thermal Dynamic Processes in Nuclear Power Plants.” Nuclear Engineering and Technology 51(6): 1540–53. <https://doi.org/10.1016/j.net.2019.04.017>.
 8. S. Arda, and K. Holbert. (2014) “Implementing a Pressurized Water Reactor Nuclear Power Plant Model into Grid Simulations.” IEEE Power and Energy Society General Meeting 2014- (October). doi:10.1109/PESGM.2014.6939303
 9. Tiwari, A. P., B. Bandyopadhyay, and G. Govindarajan. (1996) “Spatial Control of a Large Pressurized Heavy Water Reactor.” IEEE Transactions on Nuclear Science 43(4 PART 2): 2440–53.
 10. T. W. Kerlin, (1978) “Dynamic Analysis and Control of Pressurized Water Reactors,” Control and Dynamic Systems, Advances in Theory and Applications, edited by C.T. Leondes, Academic Press, vol. 14, pp. 103-212, 1978.
 11. Puchalski, B., Rutkowski, T. A., and Duzinkiewicz, K., (2017) “Nodal models of Pressurized Water Reactor core for control purposes – A comparison study,” Nuclear Engineering and Design, Vol. 322, PP. 444–463. <http://dx.doi.org/10.1016/j.nucengdes.2017.07.005>.
 12. Naghedolfeizi, M., (1990) “Dynamic Modeling of a Pressurized Water Reactor Plant for Diagnostics and Control,” Master’s Thesis, Nuclear Engineering Department, University of Tennessee.
 13. “Westinghouse Technology Systems Manual Section 1.2,” [Online]. Available:

pbadupws.nrc.gov/docs/ML1122/ML11223A195.pdf [Accessed: 12 June. 2019].

APPENDIX A

Elements of matrix A

$$\begin{aligned}
 A_{1,1} &= -\beta t / \Delta ; & A_{1,2} &= \lambda_1 ; & A_{1,3} &= \lambda_2 ; & A_{1,4} &= \lambda_3 ; & A_{1,5} &= \lambda_4 ; \\
 A_{1,6} &= \lambda_5 ; & A_{1,7} &= \lambda_6 ; & A_{1,8} &= \frac{\alpha_f}{\Delta} ; & A_{1,9} &= \frac{\alpha_c}{2\Delta} ; & A_{1,10} &= \frac{\alpha_c}{\Delta} ; \\
 A_{2,1} &= \beta_1 / \Delta ; & A_{2,2} &= -\lambda_1 ; & A_{3,1} &= \beta_2 / \Delta ; & A_{3,3} &= -\lambda_2 ; \\
 A_{4,1} &= \beta_3 / \Delta ; & A_{4,4} &= -\lambda_3 ; & A_{5,1} &= \beta_4 / \Delta ; & A_{5,5} &= -\lambda_4 ; \\
 A_{6,1} &= \beta_5 / \Delta ; & A_{6,6} &= -\lambda_5 ; & A_{7,1} &= \beta_6 / \Delta ; & A_{7,7} &= -\lambda_6 ; \\
 A_{8,1} &= \frac{F_r P_0}{(MC_p)_F} ; & A_{8,8} &= \frac{-U_{fc} * A_{fc}}{(MC_p)_F} ; & A_{8,9} &= \frac{U_{fc} * A_{fc}}{2(MC_p)_F} ; & A_{8,10} &= \frac{U_{fc} * A_{fc}}{2(MC_p)_F} ; \\
 A_{9,1} &= \frac{U_{fc} * A_{fc}}{2(MC_p)_F} ; & A_{9,1} &= \frac{(1-F_r)P_0}{(MC_p)_c} ; & A_{9,8} &= \frac{U_{fc} * A_{fc}}{(MC_p)_c} ; & A_{9,9} &= -\frac{U_{fc} * A_{fc}}{(MC_p)_c} ; \\
 A_{9,13} &= \frac{U_{fc} * A_{fc}}{(MC_p)_c} + \frac{W_{PRIM}}{M_C} ; & A_{9,13} &= \frac{W_{PRIM}}{M_C} ; & A_{10,1} &= \frac{(1-F_r)P_0}{(MC_p)_c} ; & A_{10,8} &= \frac{U_{fc} * A_{fc}}{(MC_p)_c} ; \\
 A_{10,9} &= \frac{U_{fc} * A_{fc}}{(MC_p)_c} ; & A_{10,9} &= \left[\frac{-U_{fc} * A_{fc}}{(MC_p)_c} + \frac{W_{PRIM}}{M_C} \right] ; & A_{10,10} &= -\frac{U_{fc} * A_{fc}}{(MC_p)_c} ; \\
 A_{11,10} &= \frac{W_{PRIM}}{M_C} ; & A_{11,10} &= \frac{W_{PRIM}}{M_{UP}} ; & A_{11,11} &= -\frac{W_{PRIM}}{M_{UP}} ; & A_{12,11} &= \frac{W_{PRIM}}{M_{HL}} ; \\
 A_{12,12} &= -\frac{W_{PRIM}}{M_{HL}} ; & A_{13,13} &= \frac{W_{PRIM}}{M_{LP}} ; & A_{13,14} &= \frac{W_{PRIM}}{M_{LP}} ; \\
 A_{14,14} &= \frac{W_{PRIM}}{M_{CL}}
 \end{aligned}$$

Element of matrix B

$$\begin{aligned}
 B_{1,1} &= 1 / \Delta ; & B_{14,2} &= \frac{W_{PRIM}}{M_{CL}} ; & B_{9,3} &= \left(\frac{T_{LP0} - T_{C10}}{M_C} \right) ; \\
 B_{10,3} &= \left(\frac{T_{LP0} - \Delta T_{C10}}{M_C} \right) ; & B_{11,3} &= \frac{(T_{C20} - T_{UP0})}{M_{UP}} ; & B_{12,3} &= \frac{(T_{UP0} - T_{HL0})}{M_{CL}} ; \\
 B_{13,3} &= \frac{(T_{CL0} - T_{LP0})}{M_{LP}} ; & B_{14,3} &= \frac{(T_{PSGO0} - T_{CL0})}{M_{CL}}
 \end{aligned}$$